Research Article

Lipidomics and Anti-Inflammation Activity of Brown Algae, *Lobophora* sp., in Vietnam

Thu Hue Pham [ID],[1,2] **Van Tuyen Anh Nguyen** [ID],[3] **Thi Thanh Trung Do** [ID],[3] **Anh Duy Do** [ID],[4] **Duc Tien Dam** [ID],[5] **Thi Thanh Van Tran** [ID],[6] **Quoc Long Pham** [ID],[3] and **Tat Thanh Le** [ID][1,3]

[1]*Graduate Univesity of Science and Technology, Vietnam Academy of Science and Technology, Hanoi, Vietnam*
[2]*Vietnam Naval Academy, Nha Trang, Vietnam*
[3]*Institute of Natural Products Chemistry, Vietnam Academy of Science and Technology, Hanoi, Vietnam*
[4]*Research Institute for Marine Fisheries, Hai Phong, Vietnam*
[5]*Institute of Marine Environment and Resources, Vietnam Academy of Science and Technology, Hanoi, Vietnam*
[6]*Nhatrang Institute of Technology Research and Application, Vietnam Academy of Science and Technology, Hanoi, Vietnam*

Correspondence should be addressed to Tat Thanh Le; thanh.biotech@gmail.com

Lobophora sp., belonging to brown macro algae phylum, is found in coral reefs. In this study, the fatty acid composition, lipid classes, polar lipid molecular forms, and bioactivities of this algae have been determined. It follows that five classes including polar lipid (Pol), sterol (ST), free fatty acids (FFA), triacylglycerol (TAG), and hydrocarbon and wax (HW), 23 fatty acids containing 5 PUFAs (ALA, GLA, AA, EPA, and DHA) and 157 molecular types of polar lipid group containing 48 phospholipid molecular forms belonging to 4 subclasses (PI (11), PC (14), PG (22), PA (1)), 45 glycolipid molecular forms classified into 3 subclasses of MGDG (8), DGDG (1), SQDG (36), and 64 betaine lipid molecular forms belonging to 2 subclasses (DGTA (37), DGTS (27)) have been identified for the first time from this algae. Furthermore, both polar lipid (PL) and unpolar lipid (UPL) show the NO inhibition activities with values of IC_{50} ranging from 52.10 to 66.21 μg/mL. Thus, lipid of this brown algae could promise to be a potential source for application in food, cosmetic, and pharmaceutic industry.

1. Introduction

Plants produce secondary metabolites as signals to interact with the environment and stresses [1, 2]. A number of secondary metabolites from seaweeds have been detected to have such valuable bioactivities as antibacterial, anti-viral, anticancer, and antioxidant. In Vietnam, the brown seaweed genus *Lobophora* belongs to the family Dictyotaceae, found worldwide in tropical to temperate waters and discovered in the coral reef. From the early 1980s to 2017, 49 scientific works have been reported on chemicals and bioactivities of *Lobophora* genus, in which 40 have been reported with bioactivities. Particularly, most of the studies have been centered on *Lobophora variegata*, while other species have been still poorly studied and reported [3]. Until now, there have been few studies on lipidomic profile and their bioactivities.

Certain lipid classes have been identified in several algae including polar (Pol), sterol (ST), diacylglycerol (DG), free fatty acids (FFA), triacylglycerol (TG), monoalkyldiacylglycerol (MADG), and hydrocarbons and wax (HW) [4], while neutral lipid classes play various roles such as storing energy or pre-hormones for the body; the polar lipid class has been especially considered for its various bioactivities such as acting as antioxidant and helping in curing cardiovascular diseases and cancer caused by long chain polyunsaturated fatty acids (PUFAs) [5, 6]. Some high level PUFAs containing C20 fatty acids such as 20:4n-6 (AA), 20:5n-3 (EPA), and 20:3n-6 have been identified and evaluated bioactivities in 7 brown seaweed species belonging to the genera *Sargassum, Cystoseira, Padina, and Turbinaria*. Other PUFAs have been identified as 22:6n-3 (DHA), which is a highly valuable bioactive fatty acid for

application in medicine and food [7]. In addition to being sources of PUFA, the polar lipids have an important role in structural function as components of cell membranes [8].

In algae, fatty acids are found in the esterified structure such as glycoglycerolipids (GLs), glycerophospholipids (PLs), and betaine lipids [9]. The research on the lipidomics is essential to identify new bioactive compounds and properties based on the polar lipid composition [10]. Moreover, it is also a critical step to the discovery of fostering bio-prospection of lipidic extracts.

Nowadays, mass spectrometry (MS) coupled with liquid chromatography (LC) technique is usually used to determine the detailed structural characterization of lipids and to fully explore lipidomic signature of distinct matrices [11, 12] and identify lipidome signature of cultivated seaweeds *Ulva lactuca* Linnaeus [13], *Chondrus crispus* Stackhouse [14], and *Codium tomentosum* Stackhouse [15]. However, there has been no report on *Lobophora* genus lipidome.

This study aims to analyse and identify the lipid characterisation of species *Lobophora* sp. first collected at Con Dao, Ba Ria-Vung Tau, Vietnam, by using high-performance liquid chromatography in combination with high-resolution mass spectrometry (HPLC-HRMS). The lipid extracts have also been pre-tested for anti-inflammatory effects by inhibiting the production of NO.

2. Materials and Methods

The *Lobophora* sp. samples were collected in Con Dao, Ba Ria-Vung Tau, Vietnam. Chemicals were obtained from Sigma, Merck, that reached the purification standards for analysis and HPLC grade.

2.1. Total Lipid Extraction.
Total lipid was extracted according to method of Bligh and Dyer [16] and Nguyen et al. [17]. Polar lipids were obtained by the silica column. The 200 mg of total lipid was dissolved in chloroform and loaded on the silica column (Phillipsburg, NJ), washed by 44 ml chloroform to remove the pigments and neutral lipid, and then eluted by 120 ml MeOH 95% to obtain polar lipids. The obtained fractions were stored in chloroform at −5°C for analysis.

2.2. Analyses of Lipid Classes.
Total lipids were dissolved in $CHCl_3$ (10 mg/ml) and spotted on the Sorbfil thin plate (6×6 cm). The n-hexane/diethyl ether/acetic acid (85/15/1, v/v/v) solvent was applied to identify neutral lipid layers; then, the $CHCl_3/CH_3OH$ (2/1, v/v) solvent was applied to identify the polar lipid layer. The TLC was displayed by 10% H_2SO_4/CH_3OH reagent at 240°C for 10 minutes. The image of thin layer was obtained using Epson Perfection 2400 scanner, Japan, with grayscale mode. The lipid layers on the thin plate and the percentage of the layers were identified by light sensitivity on the Sorbfil TLC Analysis software Video densitometer, Krasnodar, Russia [17, 18].

2.3. Analyses of Fatty Acids.
Fatty acid methyl esters (FAMEs) were obtained by incubating total lipid with 2% H_2SO_4 in CH_3OH at 80°C for 2 hrs and then cleaned by TLC in the hexane:diethyl ether, 95/5 (v/v) solvent. FAMEs were analysed on Shimadzu GC-2010 gas chromatograph (Kyoto, Japan) using flame ionization detector (FID) on Capillary Equity 5 (Merck, $L \times ID$ 30 m $\times$ 0.25 mm, df 0.25 μm). Carrier gas was He at the speed of 20 ml/min. Temperature program in the oven operating was at 160°C, raised 2°C/min to 240°C, and then kept for 20 minutes. Fatty acids were identified by the equivalent retention time value, Equivalent Chain Length, with the standard system of fatty acids C16 : 0 and C18 : 0. The fatty acid structures were identified by GC-MS. The spectra were compared with the NIST library and fatty acid mass spectra archive [17, 18].

2.4. Analysis of Molecular Species of Polar Lipids.
The molecules of polar lipids were analysed by high-performance liquid chromatography combined high resolution mass spectrometry (HPLC-HRMS) with Shim-Pack diol column (ID 50 mm $\times$ 4.6 mm, carrier size 5 μm, Shimadzu, Kyoto, Japan). The polar lipid classes were separated by HPLC in a solvent A: n-hexane/2-propanol/formic acid/$(C_2H_5)_3N$ and the solvent B: 2-propanol/H_2O/formic acid/$(C_2H_5)_3N$ [19] and then detected by the high-resolution ion trap over time of mass spectrometry using the LC/MS-IT-TOF (Shimadzu) device, an electronic atomizing ionization source (ESI) device. Flow rate was 0.2 ml/min [17, 20, 21].

2.5. Nitric Oxide Production Inhibition Assay.
In vitro anti-inflammatory activity of lipid samples was elucidated by using nitric oxide (NO) assay as described previously by Mosmann [22] using the Griess reagents (Promega, USA). The RAW 264.7 cells at the concentration of 2×10^5 cells/mL were dropped on the 96-well plate and incubated in 37°C with 5% CO_2 in 24 h. The culture medium was exchanged to Dulbecco's Modified Eagle's Medium (DMEM) (Life Technologies, USA) with no fetal bovine serum (FBS) for 3 hours. The cells were incubated with the lipid fractions at different concentrations before stimulating the NO production by LPS (1 μg/mL) for 24 hours. Then, the amount of nitrite in the culture medium was measured by Griess reaction at room temperature for 10 minutes. The fresh culture medium was used as a blank, while L-NMMA (Sigma) was tested as the positive sample. The mixtures were quantified spectrophotometrically at 540 nm using a micro-plate reader (ELx800 Biotekm, USA). The sodium nitrite was used as a standard compound to establish the standard curve. The NO inhibition was calculated following the formula: %NO inhibition = 100% − [concentration of NO_{sample}/concentration of NO_{LPS}] ∗ 100. IC50s were calculated by TableCurve 2Dv4 software.

The cell viability test was performed parallel with the NO inhibition assay. The 3-(4,5-dimethylthiazol-2-yl)-2,5-diphenyltetrazolium bromide (MTT) was used to evaluate cell viability because active cells transform the water-soluble MTT to an insoluble purple formazan. 20 μl lipid sample and 180 μL of RAW 264.7 cells were put into 96-well plates and then incubated with 5% CO_2 for 72 hours at 37°C. After adding MTT (5 μg/mL), the mixtures were incubated for 4

hours and supernatant was removed. The formazan crystals were dissolved in DMSO and measured at 540 nm. The percentage of cell viability was determined by comparing to the control samples.

3. Results and Discussion

3.1. Total Lipid. Total lipid content from brown algae *Lobophora* sp. is $1.06 \pm 0.2\%$ weight of fresh algae, similar to the brown samples previously studied [4, 23]. Compositions and contents of total lipid classes of *Lobophora* sp. are shown in Figure 1 and Table 1. Pol class accounts for the highest level of 26.8% compared with the detected classes, following by 4 classes of TG, FFA, ST, and HW with the content of 26.0%, 25.9%, 18.5%, and 2.7%, respectively.

3.2. Fatty Acids Composition. In the lipid composition of *Lobophora* sp. (Table 2), 23 fatty acids C12–C22 are identified. SAFAs contain 8 fatty acids $12:0$, $14:0$, $15:0$, $16:0$, $17:0$, $18:0$, $20:0$, and $22:0$, in which $14:0$ (9.62%) and $16:0$ (12.04%) have high contents. MUFAs group has $16:1n-5$, $16:1n-7$, $18:1n-7$, and $18:1n-9$, in which $18:1n-9$ (11.53%) is typical. PUFAs group has 11 fatty acids including $18:2n-6$, $18:3n-3$, $18:3n-6$, $18:4n-3$, $20:2n-6$, $20:3n-6$, $20:3n-9$, $20:4n-3$, $20:4n-6$ (AA) $20:5n-3$ (EPA), and $22:6n-3$ (DHA), in which AA (12.14%), EPA (11.56%), and DHA (14.26%) are significant.

3.3. Molecular Species of Polar Lipids. Three subclasses including phospholipid, glycolipid, and betaine lipid were identified in 26.80% polar lipid (Pol).

First, the phospholipid subclass contains 4 groups of phosphatidylinositol (PI), phosphatidylcholine (PC), phosphatidylglycerol (PG), and phosphatidic acid (PA). In PI group, 13 molecular forms were found, of which 11 forms had complete formula with one PI isomer form and no alkenyl acyl glycerophosphoinositol (Table 3).

In particular, PI $34:1$ is recognized at the highest rate of 44.09% PI Figure (1S). On the MS^- spectrum, the ion $[M-H]^-$ has the strongest signal at m/z 835.5283 corresponding to ion $[C_{43}H_{79}O_{13}P]^-$ (calculated 836.5415, different 0.00620). The MS^{2-} spectrum shows signals at m/z 255.2338 corresponding to the anion of $16:0$ fatty acids and m/z 281.2471 to the anion of $18:1$ fatty acid. Importantly, fragment at m/z 297.0334 is the considered ion $[C_{43}H_{79}O_{13}P]^-$ that lost the diacyl group which is the characteristic fragmentation to determine the PI molecular forms. Thus, the mass spectrometry data prove that the considered molecule is diacyl glycerophosphoinositol PI $16:0/18:1$ or PI $34:1$.

In the PC group, 18 molecular forms have been identified, in which 14 molecular forms are completely identified with one isomer (Table 3). The PC fragmentation has been observed on both MS^- and MS^+ with signals of ions $[M+H]^+$, $[M+HCOO]^-$, and $[M-CH_3]^-$. For example, the PC $30:0$ with highest content of 19.3% is recognized with the appearance of $[M+H]^+$ signal at m/z 706.5375 corresponding to $[C_{38}H_{77}NO_8P]^+$ (calculated 705.5309, different

0.00063) and two signals at m/z 750.5226 and m/z 690.5025 corresponding to ion $[M+HCOO]^-$ and ion $[M-CH_3]^-$, respectively (Figure 2S). On the MS^{2-} spectrum, the signal at m/z 690.5088 is formed by removing a $C_2H_4O_2$ molecule (methyl formate) from the ion at m/z 750.5226. Besides, two fragments at m/z 227.2042 corresponding to ion of $14:0$ fatty acid (calculated 228.2089, different 0.00255) and at m/z 255.2262 to ion of $16:0$ fatty acid (calculated 256.2402, different 0.00675) have resulted. Therefore, PC $30:0$ has been identified as diacyl glycerophosphocholine, PC $14:0/16:0$.

In the PG group, 15 molecular forms have been determined with complete formula, in which 6 PGs are detected with isomers (Table 3). PG $34:2$ is found at the highest rate of 41.83%. On the MS^-, signal of ion $[M-H]^-$ is observed with the strongest intensity at m/z 745.4985 corresponding to ion $[C_{40}H_{74}O_{10}P]^-$. The MS^{2-} of the ion $[C_{40}H_{74}O_{10}P]^-$ (Figure 3S) contains a signal at m/z 253.2137 (calculated 254.2246, different 0.0009) corresponding to $16:1$ fatty acid and signal at m/z 281.2485 (calculated 282.2559, different 0.0026) corresponding to $18:1$ fatty acid. Besides, there have been 3 signals including at m/z 417.2395; 491.2738; 509.2838 corresponding to molecules which have lost glycerol and acyl groups of $16:1$ fatty acid anion; a $16:1$ fatty acid; a ketene group of $16:1$ fatty acid anion, respectively. In addition, the MS^{2-} (Figure 3S) shows a lower intensity signal at m/z 279.2349 (calculated 280.2402, different 0.00195) corresponding to the carboxylate anion of $18:2$ fatty acid. This indicates that there is an isomer of PG $34:2$ with composition containing $18:2$ and $16:0$ fatty acids. The above data demonstrate that the molecular ion value m/z 745.4985 presents two isomers including PG $16:0/18:2$ and PG $16:1/18:1$, in which PG $16:1/18:1$ is the major content.

With the PA molecular forms, only one PA $40:8$ is identified (Table 3). On the MS^- spectrum of PA, ion $[M-H]^-$ is observed with the strongest signal at m/z 743.4609 (calculated 744.4730, different 0.00483, 11 double bonds) corresponding to ion $[C_{43}H_{68}O_8P]^-$ (Figure 4S). On the MS^{2-}, fragments have been found with the signals at m/z 457.2260 and m/z 439.2215 corresponding to the considered PA fragment which has lost a dehydrated molecule of $20:4$ and a $20:4$ fatty acids, respectively. Additionally, the signal at m/z 303.2243 is the acyl carboxylate ion of $20:4$ fatty acid. With the above data, PA $40:8$ is identified as diacyl glycerophosphatic acid PA $20:4/20:4$.

Second, in the glycolipid subclass, 3 groups have been identified including monogalactosyldiacylglycerol (MGDG), digalactosyldiacylglycerol (DGDG), and sulfoquinovosyldiacylglycerol (SQDG). In the MGDG group, 21 molecular forms are identified, in which 8 have been completely identified (Table 4).

For example, with the highest ratio of 13.92%, MGDG $38:9$ has formed molecular ions (Figure 5S). On the MS^-, the ion $[M+HCOO]^-$ signal at m/z 841.5021 corresponds to ion $[C_{48}H_{73}O_{12}]^-$ and the ion $[M-H]^-$ signal at m/z 795.5046 corresponds to ion $[C_{47}H_{71}O_{10}]^-$. On the MS^+, the ion $[M+Na]^+$ has the strongest signal at m/z 819.5023 corresponding to $[C_{47}H_{72}O_{10}Na]^+$. On the MS^{2+} of $[C_{47}H_{72}O_{10}Na]^+$ ion, it has been simultaneously observed
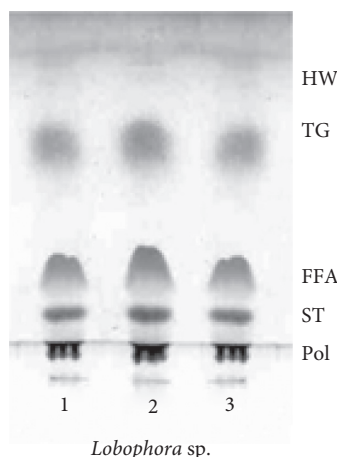
Figure 1: TLC for determination of total lipid.

Table 1: Five main classes (% of total lipid) of *Lobophora* sp.

Lipid class	Content (%)
Hydrocarbon and wax (HW)	2.7 ± 0.1
Triacylglycerol (TG)	26.1 ± 0.3
Free fatty acids (FFA)	25.9 ± 0.6
Sterols (ST)	18.5 ± 0.4
Polar lipid (Pol)	26.8 ± 0.5

Table 2: Fatty acid profile (% of total) is identified by GC through the retention time, presented with relative abundance (%) through the area of peaks.

FA	R. t (min)	Area	Content (%)
∑ SAFAs		415367.3	**22.80**
12:0	10.378	2540.9	0.14
14:0	11.79	175274.9	9.62
15:0	15.045	5711.9	0.31
16:0	18.725	219431.0	12.04
17:0	21.663	3011.5	0.17
18:0	26.624	3236.6	0.18
20:0	39.466	1788.1	0.10
22:0	53.211	4372.4	0.24
∑ MUFAs		275411.2	**15.12**
16:1n-5	18.541	20962.8	1.15
16:1n-7	17.931	36794.7	2.02
18:1n-7	25.799	10957.1	0.60
18:1n-9	25.600	206696.6	11.35
∑ PUFAs		1092787.0	**59.98**
18:2n-6	24.949	83066.0	4.56
18:3n-3	25.334	122483.9	6.72
18:3n-6	24.687	95003.7	5.21
18:4n-3	24.826	21806.6	1.20
20:2n-6	33.406	6677.5	0.37
20:3n-6	32.921	20389.4	1.12
20:3n-9	32.655	44276.1	2.43
20:4n-3	32.444	7549.2	0.41
20:4n-6 (AA)	31.944	221189.9	12.14
20:5n-3 (EPA)	32.212	210603.5	11.56
22:6n-3 (DHA)	43.138	259741.5	14.26
Other[a]		38246.8	2.10

[a]Hexadecanal, octadecenal, and fatty aldehyde are dimethylacetal derivatives determined by GC; SAFAs: saturated fatty acids; MUFAs: monounsaturated fatty acids; PUFAs: polyunsaturated fatty acids.

Table 3: Molecular species of phospholipid including PI, PC, PG, and PA groups identified by HPLC-HRMS as negative $[M - H]^-$ ion and positive $[M + H]^+$ ion, and identification as phospholipid and fatty acyl composition confirmed by the analysis of the LC-MS/MS spectra of each ion.

$[M - H]^-$ m/z	PI	Fatty acid chains	% in PI
781.4797	30:0	14:0/16:0	1.81
805.483	32:2	14:0/18:2	0.82
	32:1	14:0/18:1	6.27
807.4966		16:0/16:1	
809.5144	32:0	16:0/16:0	2.39
821.515	33:1		0.97
829.4807	34:4		1.67
831.4957	34:3	16:0/18:3	2.60
833.512	34:2	16:0/18:2	8.77
835.5283	34:1	16:0/18:1	44.09
845.5116	35:3		1.63
855.4971	36:5	16:0/20:5	1.40
857.5103	36:4	16:0/20:4	15.43
859.5269	36:3	16:0/20:3	12.15

$[M + H]^+$ m/z	PC	Fatty acid chains	% in PC
678.5056	28:0	14:0/14:0	15.33
706.5375	30:0	14:0/16:0	19.30
732.5494	32:1	14:0/18:1	6.44
		16:0/16:1	
734.5677	32:0	16:0/16:0	4.07
754.5364	34:4	14:0/20:4	7.81
756.5515	34:3	14:0/20:3	3.25
758.5678	34:2	16:0/18:2	5.84
760.5819	34:1	16:0/18:1	7.00
762.6003	34:0	14:0/20:0	1.06
768.5880	36:3		0.20
780.5566	36:5		1.69
782.5719	36:4	16:0/20:4	10.64
784.5839	36:3	16:0/20:3	5.54
786.5970	36:2	16:0/20:2	2.66
806.5627	38:4		2.21
808.5837	38:5	18:1/20:4	5.31
810.5933	38:2		1.47
838.6291	40:4		0.18

$[M - H]^-$ m/z	PG	Fatty acid chains of PG	% in PG
691.4524	30:1	14:0/16:1	0.31
693.469	30:0	14:0/16:0	0.74
717.4698	32:2	16:1/16:1	0.85
		14:1/18:1	
719.4851	32:1	16:0/16:1	4.94
721.5006	32:0	16:0/16:0	1.07
741.4682	34:4	16:1/18:3	1.38
		16:1/18:2	11.07
743.4833	34:3	16:0/18:3	
		16:2/18:1	
745.4985	34:2	16:1/18:1	41.83
		16:0/18:2	
747.5158	34:1	16:0/18:1	14.27
		18:0/16:1	
765.4675	36:6	16:1/20:5	4.68
767.482	36:5	16:0/20:5	11.22
		16:1/20:4	
769.4938	36:4	20:4/16:0	1.72
		20:3/16:1	
771.5138	36:3	16:0/20:3	1.64
773.531	36:2	18:1/18:1	3.83
793.4985	35:6	18:1/20:5	0.45

$[M - H]^-$ m/z	PA	Fatty acid chains	% in PA
743.4609	40:8	20:4/20:4	100

TABLE 4: Molecular species of glycolipid including MGDG, DGDG, and SQDG groups identified by HPLC-HRMS as negative $[M - H]^-$ ions and positive $[M + Na]^+$ ion, and identification as phospholipid and fatty acyl composition confirmed by the analysis of the LC-MS/MS spectra of each ion.

$[M + Na]^+$ m/z	MGDG	Fatty acid chains	% in MGDG
725.5160	30 : 0		1.96
747.3232	32 : 3		1.00
749.5268	32 : 2		1.75
751.5297	32 : 1	14 : 0/18 : 1	9.39
769.4902	34 : 6		1.23
771.4933	34 : 5		2.07
775.5024	34 : 3		1.81
777.5466	34 : 2		2.25
779.5654	34 : 1	16 : 0/18 : 1	13.54
793.4879	36 : 8		0.87
795.4995	36 : 7		1.56
797.5172	36 : 6		5.37
799.5326	36 : 5	16 : 0/20 : 5	7.85
801.5539	36 : 4		3.69
803.5563	36 : 3		1.71
819.5023	38 : 9	18 : 4/20 : 5	13.92
821.5147	38 : 8	18 : 3/20 : 5	13.73
823.5270	38 : 7	18 : 3/20 : 4	9.12
825.5550	38 : 6	18 : 1/20 : 5	3.64
849.3232	40 : 8	20 : 4/20 : 4	2.24
851.5628	40 : 7		1.30

$[M + Na]^+$ m/z	DGDG	Fatty acid chains	% in DGDG
941.6144	34 : 1	16 : 0/18 : 1	100

$[M - H]^-$ m/z	SQDG	Fatty acid chains	% in SQDG
737.4474	28 : 0	14 : 0/14 : 0	1.63
		12 : 0/16 : 0	
751.4631	29 : 0	14 : 0/15 : 0	0.44
763.4619	30 : 1	14 : 0/16 : 1	0.74
765.4771	30 : 0	14 : 0/16 : 0	21.78
779.4909	31 : 0	15 : 0/16 : 0	0.63
789.4757	32 : 2	14 : 0/18 : 2	0.71
791.4931	32 : 1	14 : 0/18 : 1	9.70
		16 : 0/16 : 1	
793.5107	32 : 0	16 : 0/16 : 0	13.68
815.4871	34 : 3	16 : 0/18 : 3	0.73
		14 : 0/20 : 3	
817.5065	34 : 2	16 : 0/18 : 2	3.21
		16 : 1/18 : 1	
819.5162	34 : 1	16 : 0/18 : 1	21.22
821.5376	34 : 0	16 : 0/18 : 0	5.83
		14 : 0/20 : 0	
833.5376	35 : 1	17 : 0/18 : 1	0.77
		16 : 0/19 : 1	
835.5563	35 : 0	16 : 0/19 : 0	0.10
837.4736	36 : 6	16 : 0/20 : 6	1.58
839.4834	36 : 5	16 : 0/20 : 5	2.30
841.4987	36 : 4	16 : 0/20 : 4	2.10
843.5163	36 : 3	16 : 0/20 : 3	0.45
845.5369	36 : 2	16 : 0/20 : 2	1.79
		18 : 1/18 : 1	
847.5562	36 : 1	18 : 0/18 : 1	0.61
		16 : 0/20 : 1	
849.5704	36 : 0	16 : 0/20 : 0	1.48
		18 : 0/18 : 0	
877.6017	38 : 0	16 : 0/22 : 0	0.71

TABLE 4: Continued.

$[M + Na]^+$ m/z	MGDG	Fatty acid chains	% in MGDG
		14 : 0/24 : 0	
903.6170	40 : 1	16 : 0/24 : 1	0.17
905.6325	40 : 0	16 : 0/24 : 0	4.85
931.6486	42 : 1	16 : 0/26 : 1	0.71
933.6654	42 : 0	16 : 0/26 : 0	2.08

with two signals at m/z 543.2932 and 517.2795 corresponding to the considered MGDG molecule lost fragments of m/z 276.2091 $[C_{18}H_{27}O_2]^-$ (18 : 4 fatty acid) and m/z 302.2228 $[C_{20}H_{29}O_2]^-$ (20 : 5 fatty acid), respectively. The obtained data show that the MGDG 38 : 9 is 18 : 4/20 : 5.

In the DGDG group, only one DGDG form has been found as DGDG 34 : 1 which is described in Table 4 and Figure 6S. On the MS^+ spectrum, the ion $[M + Na]^+$ has the signal at m/z 941.6144 corresponding to ion $[C_{49}H_{90}O_{15}Na]^+$. On the MS^- spectrum, the ion $[M - H]^-$ has the strongest signal at m/z 917.6080 corresponding to ion $[C_{49}H_{89}O_{15}]^-$ (calculated 917.6116, different 0.00580). On the MS^{2-} spectrum of ion $[C_{49}H_{89}O_{15}]^-$, there have been simultaneously signals at m/z 661.3696 and m/z 635.3551 corresponding to the considered DGDG molecule that has lost neutral fragments including 16 : 0 fatty acid (m/z 256.2420) and 18 : 1 fatty acid (m/z 282.2565). The above data indicate that the molecular form is DGDG 16 : 0/18 : 1.

In the SQDG group, 26 complete molecular forms have been identified with 10 isomers (Table 4). A molecule with the highest content of 21.78% is identified as SQDG 34 : 1. On the MS^- spectrum, the ion $[M - H]^-$ of SQDG 34 : 1 is observed with the strongest signal at m/z 819.5162 corresponding to ion $[C_{43}H_{79}O_{12}S]^-$ (Figure 7S). On the MS^{2-} spectrum, the signal at m/z 581.2991 is formed when the ion at m/z 819.5162 eliminates a dehydrated molecule of fatty acid 16 : 0. The signal at m/z 563.2831 has also been observed in the MS^{2-} spectrum simultaneously. This signal appears when the ion $[C_{43}H_{79}O_{12}S]^-$ loses fatty acid 16 : 0. In addition, the appearance of signal m/z 281.2489 (calculated 282.2559, different 0.00030) corresponds to anion of 18 : 1 fatty acid. Thus, data show that the obtained SQDG 34 : 1 is 16 : 0/18 : 1.

In addition to phospholipid and glycolipid classes, betaine lipid subclass includes 2 groups of DGTA and DGTS. In the DGTA group, 37 molecular forms have been identified, in which 29 forms are completely identified with 8 isomers (Table 5). Among those, DGTA 34 : 1 is the highest content of 10.20%. On the MS^+ spectrum, the ion $[M + H]^+$ has the strongest signal at m/z 738.6298 corresponding to ion $[C_{44}H_{84}NO_7]^+$. On the MS^{2+} spectrum, there have been simultaneously two signals at m/z 500.3955 and 482.3784 corresponding to the ion $[C_{44}H_{84}NO_7]^+$ that has lost a dehydrated molecule of fatty acid 16 : 0 and a neutral fragment of 16 : 0 fatty acid. Besides, the ion $[C_{44}H_{84}NO_7]^+$ has lost a dehydrated molecule of 18 : 1 fatty acid and formed a signal at m/z 474.3783. This ion eliminates water molecule and shows signal at m/z 456.3806. In addition, the signal at m/z 236.1485 is semimolecule ion of DGTA that lost diacyl groups, which is a very important signal in determining the

TABLE 5: Molecular species of betaine lipid including DGTA and DGTS groups identified by HPLC-HRMS as positive $[M + H]^+$ ion, and identification as phospholipid and fatty acyl composition confirmed by the analysis of the LC-MS/MS spectra of each ion.

$[M + H]^+$ m/z	DGTA	Fatty acid chains	% in DGTA
656.5454	28:0	14:0/14:0	1.73
682.5651	30:1	14:0/16:1	3.06
684.5841	30:0		1.33
706.5612	32:3	14:0/18:3	2.60
708.5813	32:2	14:0/18:2	9.89
710.5983	32:1	14:0/18:1	10.12
		16:0/16:1	
712.6104	32:0		0.06
724.617	33:1		0.54
728.5457	34:6	14:0/20:6	0.57
730.5541	34:5	14:0/20:5	3.67
732.5674	34:4	14:0/20:4	9.02
734.5828	34:3	14:0/20:3	5.04
		16:0/18:3	
736.6094	34:2	16:0/18:2	7.47
		14:0/20:2	
738.6298	34:1	16:0/18:1	10.20
752.6434	35:1	16:0/19:1	0.47
		17:0/18:1	
756.5699	36:6	16:0/20:6	0.88
758.5821	36:5	16:0/20:5	1.83
760.6001	36:4	16:0/20:4	6.17
762.6193	36:3	16:0/20:3	7.39
		18:1/18:2	
764.6342	36:2		4.33
766.6548	36:1	18:0/18:1	1.40
		16:0/20:1	
782.5867	38:7		0.37
784.6011	38:6	18:2/20:4	1.63
786.6138	38:5	18:1/20:4	2.13
788.6306	38:4	18:1/20:3	1.03
790.6501	38:3	18:0/20:3	0.68
		18:1/20:2	
792.6621	38:2		0.27
794.6813	38:1	18:1/20:0	0.20
804.5707	40:10	20:4/20:6	0.49
806.5888	40:9	20:4/20:5	0.52
808.6031	40:8	20:4/20:4	1.45
810.617	40:7	20:3/20:4	1.72
812.6332	40:6	20:2/20:4	0.98
		20:3/20:3	
814.6478	40:5	20:1/20:4	0.44
		20:2/20:3	
848.6329	43:9		0.32
$[M + H]^+$ m/z	DGTS	Fatty acid chains	% in DGTS
656.5455	28:0	14:0/14:0	19.21
682.5609	30:1	14:0/16:1	1.34
		14:1/16:0	
684.5776	30:0	14:0/16:0	9.71
706.5524	32:3	14:0/18:3	3.25
708.5767	32:2	14:0/18:2	4.78
		16:0/16:2	
710.5923	32:1	14:0/18:1	12.14
		16:0/16:1	
712.6104	32:0	16:0/16:0	5.03
		14:0/18:0	
724.6059	33:1		1.80

TABLE 5: Continued.

$[M + H]^+$ m/z	DGTA	Fatty acid chains	% in DGTA
730.5586	34:5		1.82
732.5736	34:4	16:0/18:4	5.20
		14:0/20:4	
		16:1/18:3	
734.5875	34:3	16:0/18:3	5.15
		14:0/20:3	
		16:1/18:2	
736.6072	34:2	16:0/18:2	7.29
		16:1/18:1	
738.6226	34:1	16:0/18:1	12.20
752.634	35:1		1.30
756.576	36:6		1.55
758.5891	36:5		1.07
760.6036	36:4	16:0/20:4	3.39
		18:1/18:3	
762.6204	36:3		2.62
764.6344	36:2	18:1/18:1	4.76
		16:0/20:2	
		18:0/18:2	
766.6518	36:1		1.24
784.6068	38:6		1.54
786.6186	38:5	18:1/20:4	1.52
		16:0/22:5	
788.6389	38:4		0.63

molecular forms of DGTA (Figure 8S). Thus, the above data prove that the considered molecule is DGTA 16:0/18:1.

There are 23 molecular forms with 13 isomers identified in DGTS subclass (Table 5). The DGTS molecular form at the highest ratio of 19.21% is DGTS 28:0. On the MS^+ spectrum, the ion $[M + H]^+$ has the strongest signal at m/z 656.5459 corresponding to ion $[C_{38}H_{74}NO_7]^+$ (Figure 9S). On the MS^{2+} spectrum, signal at m/z 446.3490 appears because the ion $[C_{38}H_{74}NO_7]^+$ loses a dehydrated molecule of acid 14:0. Signal at m/z 428.3395 has also been observed in the MS^{2+} spectrum. This signal corresponds to the ion $[C_{38}H_{74}NO_7]^+$ that loses a neutral fragment of 14:0 fatty acid. In addition, the appearance of signal at m/z 236.1517 is important for detection of the molecular form of DGTS. It is similar to the determination of DGTA. Thus, the above data prove that the considered molecule is DGTS 14:0/14:0.

3.4. Anti-Inflammatory Activity. Three lipid fractions yield the inhibitory effects on NO production in RAW 264.7 cells. The IC_{50} values have been evaluated from 52.10 to 66.21 μg/mL (Table 6). The unpolar lipid fraction (UPol) has a strongest activity IC_{50} of 52.10 ± 4.43, following by total lipid and polar lipid samples with IC_{50} of 61.09 ± 6.06 and 66.21 ± 6.24 μg/mL, respectively. All fractions do not exhibit the cytotoxicity with the cell viability from 96.06 to 100% at the concentration of 100 μg/mL, while the control sample shows the cell viability percentage of 89.90% with the same concentration (Table 6).

4. Discussion

In the total lipid of *Lobophora* sp., 5 classes including Pol, ST, FFA, TG, and HW have been found, while other brown algae

TABLE 6: The NO inhibition and the cell viability of lipid samples.

Concentration (μg/mL)	L-NMMA		Pol		UPol		TL	
	Cell viability	NO inhibition	Cell viability	NO inhibition	Cell viability	NO inhibition	Cell viability	NO inhibition
100	89.90	99.74	97.29	69.07	98.24	84.75	96.06	80.93
20	97.54	72.44	98.00	18.47	102.00	20.76	99.47	15.25
4	NA	28.18	NA	4.66	NA	7.20	NA	5.86
0.8	NA	9.74	NA	-1.29	NA	-3.61	NA	-2.82
IC$_{50}$		8.90 ± 0.82		66.21 ± 6.24		52.10 ± 4.43		61.09 ± 6.06

NA: not affected.

samples from the genus *Sargassum* collected in Vietnam show three or four classes of Pol, ST, FFA, and TG [4, 23]. In contrast to terrestrial plants with high content of 16C and 18C fatty acids, *Lobophora* sp. has low content of 16C and 18C fatty acids similar to brown seaweeds reported [4]. Particularly, lipid composition of *Lobophora* sp. contains a variety of fatty acids (23 types) including many long chains and 6 double bonds fatty acids belonging to ω3 (n-3) and ω6 (n-6) with 23.40% and 34.15% of the total FA, respectively. They have been considered to be beneficial for the human brain and overall health, including cardiovascular effects, improving the function of the heart and the liver, reducing blood pressure, anti-thrombosis, and helping with arthritis, cancer, and lung diseases [24–28]. Among those, α- and γ-linolenic acids (C18 : 3n-3-ALA and C18 : 3n-6-GLA) have the total content of 11.93%, which are very important fatty acids in the formation and protection of the skin to potentially apply in the cosmetic industry [29].

Previous research has shown that the fatty acid composition in seaweed contains saturated fatty acids (SFAs) with high content and polyunsaturated fatty acids (MUFAs, PUFAs) with very low content. For example, the green algae *Ulva rigida* has 64.5% SFAs, 23.78% PUFAs, and 11.71% MUFAs [9]. The brown algae *Padina pavonica* has those with content of 43.45%, 1.7%, and 23.67%, respectively [30]; some red algae species belonging to Hypnea genus in Vietnam had the content of SFAs >60%, PUFAs from 3–12%, and MUFAs is 8.55–27.88% [31]; other red algae have the similar fatty acid profile [32, 33]. Interestingly, the fatty acid profile of this *Lobophora* sp. revealed the high level of polyunsaturated fatty acids (MUFAs, PUFAs) with the content of 75.10%, which is extremely noteworthy to further study for potential application.

Lobophora sp. is an infrequent species that has been detected with 6 PUFAs belonging to the C20 fatty acid group including C20 : 2n-6; C20 : 3n-6 (DGLA); C20 : 3n-9; C20 : 4n-3; C20 : 4n-6 (AA); C20 : 5n-3 (EPA), in which DGLA, AA and EPA have content of 1.12%, 12.14%, and 11.56%, respectively. They are precursors which provide the initial fatty acids for the biosynthesis process of eicosanoids. Those are signaling molecules that control many systems in the human body, of which the most important roles are involved in the inflammatory process, immune response, and the effect on the central nervous system [33–35].

Particularly, the fatty acid C22 : 6n-3 (DHA) has been identified in the total lipid of this species with the content of 14.26% which is a valuable fatty acid in foods that helps increase the brain development of children and young animals [36]. DHA content of this species is much higher than that of other brown seaweeds collected in Vietnam and of oysters, fish, and corals [4, 18, 35]. This can be a sign to distinguish seaweeds living in coral reefs from those living in coastal areas.

Recent researches on lipid usually have applied GC-MS, GC-FID techniques to detect the composition and content of fatty acids; however, fatty acids exist in both free and linked types. Nowadays, the application of HR-MS technique helps identify the hold of lipid molecules and even molecular species based on ion values of MS [17, 18, 21]. Some novel techniques such as LC-MS/MS have been applied to study the lipidome of seaweed [9, 10, 14, 15, 37]. With HPLC-HRMS technique, 157 polar lipids molecular forms have been, for the first time, identified belonging to phospholipids, glycolipids, and betaine lipids of *Lobophora* sp.

Betaine lipids are an amphoteric subclass like phospholipids because they have a positively charged ammonium group. They are determined to have a function similar to phospholipids in many algae, fungi, and seedless plants [38–42]. DGTA is a glycerol-lipid that contains two fatty acids esterified with glycerol and an ether-linked polar group derived from an amino acid, while DGTS is an isomer structure and biosynthetic precursor of DGTA in the algae [43, 44]. The coexistence of DGTS and DTGA in many types of algae can be explained by a partial conversion of DGTS to DGTA.

In addition to molecular species analysis, the total lipid from *Lobophora* sp. has been separated into polar lipid and unpolar lipid fractions, in which polar lipid contained phospholipid, betaine lipid, and glycolipid classes. In recent studies, the extracts from *Lobophora* species have been reported on such bioactivities as anti-oxidant, anti-inflammation, anti-microbial, and cytotoxic activities [3]. In this study, we have preliminarily screened the anti-inflammation activity of three lipid fractions through the NO production inhibition assay because NO is a key signaling molecule in the inflammation process [45]. The results show that the lipid fractions exhibited the strong NO production inhibition activity.

Particularly, the unpolar lipid fraction displays a higher NO inhibitory activity than polar lipid. This result contrasts with what has been reported on lipid fraction from a mud crab *Scylla paramamosain*, which shows the inhibition of the polar lipid higher than the unpolar lipid fraction [19]. This may be caused by the polar lipid content

of *Lobophora* sp. which is lower than that of the mud crab *S. paramamosain*, 26.8% and 40.02%, respectively. Other authors have demonstrated that an abundance of PUFAs in seaweed composition related to the display of anti-inflammatory activity [9, 46]. It has also been reported that anti-inflammatory activities (IC$_{50}$) of seafood range from 64.6 to 306.4 μg/mL. In this report, the NO inhibition activity of lipid fractions is comparable to those of *Octopus* lipids [47] and sulfated polysaccharide of the marine brown algae *Lobophora variegata* [48]. Particularly, it is the first time that the *Lobophora* sp. lipid fractions have been demonstrated strong NO inhibition activity.

The recent reports indicate that the production of NO is increased by neuronal nitric oxide synthase (nNOS) mediated by the NF-κB factor [49]. In addition, the transcription of Nf-κB has been regulated by n-3 PUFAs [50]. Also, the report of Echeverria shows that n-3 PUFAs (especially EPA and DHA) partially reduce the proinflammatory indexes such as NF-κB and Nrf2 [51]. Thus, it suggests that lipid fractions containing n-3 PUFAs may inhibit NO inhibition through regulation of factors NF-κB and Nrf2.

In several expert studies, total extracts, their fractions, and molecular species have demonstrated bioactivities [52–56]. Particularly, glycolipids from different algae species have anti-viral, antibacterial, and anti-tumoral activity [53, 54]. SQDG (32 : 0) and SQMG (16 : 0) are both described to have anti-microbial activity [55, 56]. Some reports suggest that DGTS has the same function as PC due to their similar zwitterionic structure, and they are interchangeable in the cell [44]. It is significant that the MGDG displays anti-inflammatory activity and is combined with omega-3 to treat the regeneration of articular cartilage in the osteoarthritis adult. Thus, further study will be focusing on evaluating the bioactivities of the composition of *Lobophora* sp. lipid such as fatty acids, lipid classes, and molecular species.

5. Conclusions

In summary, lipid classes and fatty acid profile of seaweed *Lobophora* sp. have been well defined. The simultaneous detection of high-value long-chain polyunsaturated fatty acids such as AA, EPA, and DHA in this seaweed has inspired researches to study the origin of these fatty acids in the reef ecosystem. HPLC-HRMS technique has allowed identifying 157 molecular forms in polar lipid that are classified into betaine lipid, glycolipid, and phospholipid groups with 64, 45, and 48 molecular forms, respectively. The NO inhibition effects of lipid fractions including total lipid, polar lipid, and unpolar lipid have been reported for the first time with IC$_{50}$ from 52.10 to 66.21 μg/mL. These all suggest that *Lobophora* sp. lipids need to be further studied for potential application in food, medicine, and cosmetics.

Data Availability

No data were used to support this study.

Conflicts of Interest

The authors declare no conflicts of interest.

Supplementary Materials

Figure 1S. HPLC-HRMS and fragmentations of PI 34:1 [$C_{43}H_{79}O_{13}P$]$^-$. (a) HPLC-HRMS chromatogram of [$C_{43}H_{79}O_{13}P$]$^-$. (b) Negative mass spectrometry (MS$^-$) of [$C_{43}H_{79}O_{13}P$]$^-$. (c) Negative mass spectrometry (MS^{2-}) of signal at m/z 835.5283. Figure 2S. HPLC-HRMS and fragmentations of PC 30:0 [$C_{38}H_{77}NO_8P$]$^+$. (a) HPLC-HRMS chromatogram of [$C_{38}H_{77}NO_8P$]$^+$. (b) Positive mass spectrometry (MS$^+$) of signal at m/z [$C_{38}H_{77}NO_8P$]$^+$. (c) Negative mass spectrometry (MS$^-$) of signal at m/z 690.5025 and m/z 750.5026. (c) Negative mass spectrometry (MS^{2-}) of signal at m/z 690.5025. Figure 3S. HPLC-HRMS and fragmentations of PG 34:2 [$C_{40}H_{74}O_{10}P$]$^-$. (a) HPLC-HRMS chromatogram of [C40H74O10P]$^-$. (b) Negative mass spectrometry (MS$^-$) of [C40H74O10P]$^-$. (c) Negative mass spectrometry (MS^{2-}) of signal at m/z 745.4985. Figure 4S. HPLC-HRMS and fragmentations of PA 40:8 [$C_{43}H_{68}O_8P$]$^-$. (a) HPLC-HRMS chromatogram of [C43H68O8P]$^-$. (b) Negative mass spectrometry (MS$^-$) of [C43H68O8P]$^-$. (c) Negative mass spectrometry (MS^{2-}) of signal at m/z 743.4609. Figure 5S. HPLC-HRMS and fragmentations of MGDG 38:9 [$C_{47}H_{72}O_{10}Na$]$^+$. (a) HPLC-HRMS chromatogram of [C47H72O10Na]$^+$. (b) Positive mass spectrometry (MS$^+$) of [C47H72O10Na]$^+$. (c) Negative mass spectrometry (MS$^-$) of signal at m/z 795.5046 and m/z 841.5021. (d) Positive mass spectrometry (MS^{2+}) of signal at m/z 819.5023. Figure 6S. HPLC-HRMS and fragmentations of DGDG 34:1 [$C_{49}H_{89}O_{15}$]$^-$. (a) HPLC-HRMS chromatogram of [C49H89O15]$^-$. (b) Negative mass spectrometry (MS$^-$) of [C49H89O15]$^-$. (c) Negative mass spectrometry (MS$^-$) of [C49H89O15Na]$^+$. (d) Negative mass spectrometry (MS^{2-}) of m/z 917.600. Figure 7S. HPLC-HRMS and fragmentations of SQDG 34:1 [$C_{43}H_{79}O_{12}S$]$^-$. (a) HPLC-HRMS chromatogram of [C43H79O12S]$^-$. (b) Negative mass spectrometry (MS$^-$) of [C43H79O12S]$^-$. (c) Negative mass spectrometry (MS^{2-}) of signal at m/z 819.5162. Figure 8S. HPLC-HRMS and fragmentations of DGTA 34:1 [$C_{44}H_{84}NO_7$]$^+$. (a) HPLC-HRMS chromatogram of [C44H84NO7]$^+$. (b) Positive mass spectrometry (MS$^+$) of [C44H84NO7]$^+$. (c) Positive mass spectrometry (MS^{2+}) of signal at m/z 738.6298. Figure 9S. HPLC-HRMS

and fragmentations of DGTS 28 : 0 $[C_{38}H_{74}NO_7]^+$. (a) HPLC-HRMS chromatogram of $[C38H74NO7]^+$. (b) Positive mass spectrometry (MS^+) of $[C38H74NO7]^+$. (c) Positive mass spectrometry (MS^{2+}) of signal at m/z 656.5459. . (*Supplementary Materials*)

References

[1] A. Kumar, M. Memo, and A. Mastinu, "Plant behaviour: an evolutionary response to the environment?" *Plant Biology*, vol. 22, no. 6, pp. 961–970, 2020.

[2] A. Mahdavi, P. Moradi, and A. Mastinu, "Variation in terpene profiles of *Thymus vulgaris* in water deficit stress response," *Molecules*, vol. 25, no. 5, p. 1091, 2020.

[3] C. Vieira, J. Gaubert, O. De Clerck, C. Payri, G. Culioli, and O. P. Thomas, "Biological activities associated to the chemodiversity of the brown algae belonging to genus Lobophora (Dictyotales, Phaeophyceae)," *Phytochemistry Reviews*, vol. 16, no. 1, pp. 1–17, 2017.

[4] T. H. Pham, V. T. A. Nguyen, T. C. B. Nguyen, D. T. Dam, T. T. Le, and Q. L. Pham, *Research on the Content of Lipid Classes and Fatty Acids from Sargassum Seaweed*, in *Proceedings of ASAM conferences in Vietnam*, Hanoi, Vietnam, September 2017.

[5] K. J. Bowen, W. S. Harris, and P. M. Kris-Etherton, "Omega-3 fatty acids and cardiovascular disease: are there benefits?" *Current Treatment Options in Cardiovascular Medicine*, vol. 18, no. 11, pp. 18–69, 2016.

[6] K. H. M. Cardozo, T. Guaratini, M. P. Barros et al., "Metabolites from algae with economical impact," *Comparative Biochemistry and Physiology Part C: Toxicology & Pharmacology*, vol. 146, no. 1-2, pp. 60–78, 2007.

[7] S. Eko, S. F. Akhmad, A. Masayuki, H. Masashi, and M. Kazuo, "Lipids, fatty acids, and fucoxanthin content from temperate and tropical brown seaweeds," *Aquatic Procedia*, vol. 7, pp. 66–75, 2016.

[8] I. A. Guschina and J. L. Harwood, "Lipids and lipid metabolism in eukaryotic algae," *Progress in Lipid Research*, vol. 45, no. 2, pp. 160–186, 2006.

[9] D. Lopes, A. S. P. Moreira, F. Rey et al., "Lipidomic signature of the green macroalgae Ulva rigida farmed in a sustainable integrated multi-trophic aquaculture," *Journal of Applied Phycology*, vol. 31, no. 2, pp. 1369–1381, 2019.

[10] E. Costa, P. Domingues, T. Melo et al., "Lipidomic signatures reveal seasonal shifts on the relative abundance of high-valued lipids from the Brown algae fucus vesiculosus," *Marine Drugs*, vol. 17, no. 6, p. 335, 2019.

[11] H. He, R. P. Rodgers, A. G. Marshall, and C. S. Hsu, "Algae polar lipids characterized by online liquid chromatography coupled with hybrid linear quadrupole ion trap/fourier transform ion cyclotron resonance mass spectrometry," *Energy & Fuels*, vol. 25, no. 10, pp. 4770–4775, 2011.

[12] I. Naumann, K. H. Darsow, C. Walter, H. A. Lange, and R. Buchholz, "Identification of sulfoglycolipids from the alga Porphyridium purpureum by matrix-assisted laser desorption/ionisation quadrupole ion trap time-of-flight mass spectrometry," *Rapid Communications in Mass Spectrometry*, vol. 21, no. 19, pp. 3185–3192, 2007.

[13] P. Kumari, M. Kumar, C. R. K. Reddy, and B. Jha, "Nitrate and phosphate regimes induced lipidomic and biochemical changes in the intertidal macroalga Ulva lactuca (Ulvophyceae, Chlorophyta)," *Plant and Cell Physiology*, vol. 55, no. 1, pp. 52–63, 2014.

[14] T. Melo, E. Alves, V. Azevedo et al., "Lipidomics as a new approach for the bioprospecting of marine macroalgae-unraveling the polar lipid and fatty acid composition of Chondrus crispus," *Algal Research*, vol. 8, pp. 181–191, 2015.

[15] E. Costa, T. Melo, A. S. P. Moreira et al., "Decoding bioactive polar lipid profile of the macroalgae Codium tomentosum from a sustainable IMTA system using a lipidomic approach," *Algal Research*, vol. 12, pp. 388–397, 2015.

[16] E. G. Bligh and W. J. Dyer, "A rapid method of total lipid extraction and purification," *Canadian Journal of Biochemistry and Physiology*, vol. 37, no. 1, pp. 911–917, 1959.

[17] T. P. L. Nguyen, V. T. A. Nguyen, T. T. T. Do, Q. T. Nguyen, Q. L. Pham, and T. T. Le, "Fatty acid composition, phospholipids molecules and bioactivities of lipids of the mud crab Scylla paramamosain," *Journal of Chemistry*, vol. 2020, Article ID 8651453, 9 pages, 2020.

[18] Q. T. Tran, T. T. T. Le, M. Q. Pham et al., "Fatty acid, lipid classes and phospholipid molecular species composition of the marine clam Meretrix lyrata (Sowerby 1851) from Cua Lo beach, Nghe an province, Vietnam," *Molecules*, vol. 24, pp. 895–901, 2019.

[19] S. Harrabi, W. Herchi, H. Kallel, P. Mayer, and S. Boukhchina, "Liquid chromatographic-mass spectrometric analysis of glycerophospholipids in corn oil," *Food Chemistry*, vol. 114, no. 2, pp. 712–716, 2009.

[20] S. Boukhchina, K. Sebai, A. Cherif, H. Kallel, and P. M. Mayer, "Identification of glycerophospholipids in rapeseed, olive, almond, and sunflower oils by LC–MS and LC–MS–MS," *Canadian Journal of Chemistry*, vol. 82, no. 7, pp. 1210–1215, 2004.

[21] A. B. Imbs, V. G. Rybin, V. I. Kharlamenko et al., "Polyunsaturated molecular species of galactolipids: markers of zooxanthellae in a symbiotic association of the soft coral Capnella sp. (Anthozoa: Alcyonacea)," *Russian Journal of Marine Biology*, vol. 41, no. 6, pp. 461–467, 2015.

[22] T. Mosmann, "Rapid colorimetric assay for cellular growth and survival: application to proliferation and cytotoxicity assays," *Journal of Immunological Methods*, vol. 65, no. 1-2, pp. 55–63, 1983.

[23] B. J. Gosch, M. Magnusson, N. A. Paul, and R. De Nys, "Total lipid and fatty acid composition of seaweeds for the selection of species for oil-based biofuel and bioproducts," *GCB Bioenergy*, vol. 4, no. 6, pp. 919–930, 2012.

[24] P. J. Gillies, W. S. Harris, and P. M. Kris-Etherton, "Omega-3 fatty acids in food and pharma: the enabling role of biotechnology," *Current Atherosclerosis Reports*, vol. 13, no. 6, pp. 467–473, 2011.

[25] D. Mozaffarian and J. H. Y. Wu, "Omega-3 fatty acids and cardiovascular disease," *Journal of the American College of Cardiology*, vol. 58, no. 20, pp. 2047–2067, 2011.

[26] H. Poudyal, S. K. Panchal, L. C. Ward, and L. Brown, "Effects of ALA, EPA and DHA in high-carbohydrate, high-fat diet-induced metabolic syndrome in rats," *The Journal of Nutritional Biochemistry*, vol. 24, no. 6, pp. 1041–1052, 2013.

[27] G. P. Eckert, U. Lipka, and W. E. Muller, "Omega-3 fatty acids in neurodegenerative diseases: focus on mitochondria," *Prostaglandins, Leukotrienes and Essential Fatty Acids*, vol. 88, no. 1, pp. 105–114, 2013.

[28] Z.-Y. Liu, D.-Y. Zhou, Z.-X. Wu et al., "Extraction and detailed characterization of phospholipid-enriched oils from six species of edible clams," *Food Chemistry*, vol. 239, pp. 1175–1181, 2018.

[29] T.-H. Huang, P.-W. Wang, S.-C. Yang, W.-L. Chou, and J.-Y. Fang, "Cosmetic and therapeutic applications of fish oil's

fatty acids on the skin," *Marine Drugs*, vol. 16, no. 8, p. 256, 2018.

[30] G. Bernardini, M. Minetti, G. Polizzotto, M. Biazzo, and A. Santucci, "Pro-apoptotic activity of French polynesian Padina pavonica extract on human osteosarcoma cells," *Marine Drugs*, vol. 16, no. 12, p. 504, 2018.

[31] T. T. Le, V. T. A. Nguyen, T. H. Nguyen et al., "Survey lipid content and composition of fatty acids from Hypnea seaweed," *Vietnam Journal of Chemistry*, vol. 51, pp. 49–53, 2013.

[32] B. D. A. Daniel, C. D. Jaécio, A. S. R. Simone et al., "Fatty acid composition from the marine red algae *Pterocladiella capillacea* (S. G. Gmelin) Santelices & Hommersand 1997 and *Osmundaria obtusiloba* (C. Agardh) R. E. Norris 1991 and its antioxidant activity," *Anais da Academia Brasileira de Ciências*, vol. 90, pp. 449–459, 2018.

[33] T. T. Le, *Filter research, isolation, and identification active fatty acid, arachidonic acid and prostaglandin from red seaweed*, PhD thesis in Chemistry, Archived at GUST, VAST, 2015.

[34] S. V. Khotimchenko and V. E. Vaskovsky, "Distribution of C20 polyenoic fatty acids in red macrophytic algae," *Botanica Marina*, vol. 33, pp. 525–528, 1990.

[35] T. P. L. Dang, *Study on lipid composition and molecular forms of phospholipids from some soft corals in Vietnam*, PhD thesis in Chemistry, Archived at GUST, VAST, 2016.

[36] Q. L. Pham and V. M. Chau, *Biologically Active Lipids and Fatty Acids from Nature*pp. 100–213, Science and Technology Publising House, Hanoi, Vietnam, 1 edition, 2005.

[37] E. Costa, T. Melo, A. S. P. Moreira et al., "Valorization of lipids from *Gracilaria sp.* through lipidomics and decoding of antiproliferative and anti-inflammatory activity," *Marine Drugs*, vol. 15, pp. 1–17, 2017.

[38] W. Eichenberger and M. Hofmann, "Metabolism and distribution of betaine lipids in algae," *Metabolism, Structure and Utilization of Plant Lipids*", pp. 18–21, Centre National Pédagogique, Montffeury, Tunesie, 1992.

[39] V. E. Vaskovsky, S. V. Khotimchenko, and E. M. Boolugh, "Distribution of diacylglycerotrimethylhomoserine and phosphatidylcholine in mushrooms," *Phytochemistry*, vol. 47, no. 5, pp. 755–760, 1998.

[40] R. M. Klug and C. Benning, "Two enzymes of diacylglyceryl-O-4'-(N,N,N,-trimethyl)homoserine biosynthesis are encoded by btaA and btaB in the purple bacterium Rhodobacter sphaeroides," *Proceedings of the National Academy of Sciences*, vol. 98, no. 10, pp. 5910–5915, 2001.

[41] W. R. Riekhof, C. Andre, and C. Benning, "Two enzymes, BtaA and BtaB, are sufficient for betaine lipid biosynthesis in bacteria," *Archives of Biochemistry and Biophysics*, vol. 441, no. 1, pp. 96–105, 2005.

[42] O. A. Rozenstvet, S. V. Saksonov, V. R. Filin, and V. M. Dembitsky, "Seasonal changes of lipid content in the leaves of some ferns," *Physiologia Plantarum*, vol. 113, no. 1, pp. 59–63, 2001.

[43] K. Künzler and W. Eichenberger, "Betaine lipids and zwitterionic phospholipids in plants and fungi," *Phytochemistry*, vol. 46, no. 5, pp. 883–892, 1997.

[44] A. Vieler, C. Wilhelm, R. Goss, R. Süß, and J. Schiller, "The lipid composition of the unicellular green alga Chlamydomonas reinhardtii and the diatom Cyclotella meneghiniana investigated by MALDI-TOF MS and TLC," *Chemistry and Physics of Lipids*, vol. 150, no. 2, pp. 143–155, 2007.

[45] J. N. Sharma, A. Al-Omran, and S. S. Parvathy, "Role of nitric oxide in inflammatory diseases," *Inflammopharmacology*, vol. 15, no. 6, pp. 252–259, 2007.

[46] A. H. Banskota, R. Stefanova, S. Sperker, R. Melanson, J. A. Osborne, and S. J. B. O'Leary, "Five new galactolipids from the freshwater microalga Porphyridium aerugineum and their nitric oxide inhibitory activity," *Journal of Applied Phycology*, vol. 25, no. 4, pp. 951–960, 2013.

[47] T. Ahmad, D. Rudd, M. Kotiw, L. Liu, and K. Benkendorff, "Correlation between fatty acid profile and anti-inflammatory activity in common Australian seafood by-products," *Marine Drugs*, vol. 17, no. 3, pp. 155–174, 2019.

[48] R. C. L. Siqueira, M. S. J. da Silva, A. d. F. Pires et al., "In vivo anti-inflammatory effect of a sulfated polysaccharide isolated from the marine brown algae Lobophora variegata," *Pharmaceutical Biology*, vol. 49, no. 2, pp. 167–174, 2011.

[49] G. Rathnasamy, V. Sivakumar, P. Rangarajan, W. S. Foulds, E. A. Ling, and C. Kaur, "NF-κB-Mediated nitric oxide production and activation of caspase-3 cause retinal ganglion cell death in the hypoxic neonatal retina," *Investigative Opthalmology & Visual Science*, vol. 55, no. 9, pp. 5878–5889, 2014.

[50] R. Valenzuela and L. A. Videla, "Impact of the Co-administration of N-3 fatty acids and olive oil components in preclinical nonalcoholic fatty liver disease models: a mechanistic view," *Nutrients*, vol. 12, no. 2, pp. 499–512, 2020.

[51] F. Echeverría, R. Valenzuela, A. Espinosa et al., "Reduction of high-fat diet-induced liver proinflammatory state by eicosapentaenoic acid plus hydroxytyrosol supplementation: involvement of resolvins RvE1/2 and RvD1/2," *The Journal of Nutritional Biochemistry*, vol. 63, pp. 35–43, 2019.

[52] A. K. Gupta, M. A. Ratherme)"[?--]>, A. Kumar Jha et al., "Artocarpus lakoocha Roxb. and Artocarpus heterophyllus Lam. flowers: new sources of bioactive compounds," *Plants*, vol. 9, no. 10, p. 1329, 2020.

[53] E. Plouguerné, B. A. P. Da Gama, R. C. Pereira, and E. Barreto-Bergter, "Glycolipids from seaweeds and their potential biotechnological applications," *Frontiers in Cellular and Infection Microbiology*, vol. 4, pp. 1–5, 2014.

[54] J. W. Blunt, B. R. Copp, R. A. Keyzers, M. H. G. Munro, and M. R. Prinsep, "Marine natural products," *Natural Product Reports*, vol. 33, no. 3, pp. 382–431, 2016.

[55] F. K. El Baz, G. S. El Baroty, H. H. Abd El Baky, O. I. Abd El Salam, and E. A. Ibrahim, "Structural characterization and biological activity of sulfolipids from selected marine algae," *Grasas y Aceites*, vol. 64, pp. 561–571, 2013.

[56] H. Wang, Y. L. Li, W. Z. Shen, W. Rui, X. J. Ma, and Y. Z. Cen, "Antiviral activity of a sulfoquinovosyldiacylglycerol (SQDG) compound isolated from the green alga *Caulerpa racemosa*," *Botanica Marina*, vol. 50, pp. 185–190, 2007.